EBioMedicine 31 (2018) 122–132

Contents lists available at ScienceDirect

EBioMedicine

journal homepage: www.ebiomedicine.com

Research Paper

Activation of Liver AMPK with PF-06409577 Corrects NAFLD and Lowers Cholesterol in Rodent and Primate Preclinical Models

Ryan M. Esquejo [a], Christopher T. Salatto [a], Jake Delmore [a], Bina Albuquerque [a], Allan Reyes [a], Yuji Shi [a], Rob Moccia [b], Emily Cokorinos [a], Matthew Peloquin [a], Mara Monetti [a], Jason Barricklow [c], Eliza Bollinger [a], Brennan K. Smith [d], Emily A. Day [d], Chuong Nguyen [e], Kieran F. Geoghegan [e], John M. Kreeger [f], Alan Opsahl [f], Jessica Ward [a], Amit S. Kalgutkar [g], David Tess [g], Lynne Butler [f], Norimitsu Shirai [f], Timothy F. Osborne [g], Gregory R. Steinberg [d], Morris J. Birnbaum [a], Kimberly O. Cameron [h], Russell A. Miller [a,*]

[a] Internal Medicine Research Unit, Pfizer Inc, Cambridge, MA, USA
[b] Computational Sciences, Pfizer Inc, Cambridge, MA, USA
[c] Pharmacokinetics, Dynamics, and Metabolism, Pfizer Inc, Groton, CT, USA
[d] Division of Endocrinology and Metabolism, Department of Medicine and Department of Biochemistry and Biomedical Sciences, McMaster University, 1280 Main St. W., Hamilton, ON L8N 3Z5, Canada
[e] Primary Pharmacology Group, Pfizer Inc, Groton, CT, USA
[f] Drug Safety Research and Development, Pfizer Inc, Groton, CT, USA
[g] Sanford Burnham Prebys Medical Discovery Institute, 6400 Sanger Road, Orlando, FL 32827, USA
[h] Medicine Design, Pfizer Inc, Cambridge, MA

ARTICLE INFO

Article history:
Received 8 December 2017
Received in revised form 26 March 2018
Accepted 6 April 2018
Available online 8 April 2018

Keywords:
AMPK
NAFLD
Lipogenesis
ACC
Hyperlipidemia

ABSTRACT

Dysregulation of hepatic lipid and cholesterol metabolism is a significant contributor to cardiometabolic health, resulting in excessive liver lipid accumulation and ultimately non-alcoholic steatohepatitis (NASH). Therapeutic activators of the AMP-Activated Protein Kinase (AMPK) have been proposed as a treatment for metabolic diseases; we show that the AMPK β1-biased activator PF-06409577 is capable of lowering hepatic and systemic lipid and cholesterol levels in both rodent and monkey preclinical models. PF-06409577 is able to inhibit *de novo* lipid and cholesterol synthesis pathways, and causes a reduction in hepatic lipids and mRNA expression of markers of hepatic fibrosis. These effects require AMPK activity in the hepatocytes. Treatment of hyperlipidemic rats or cynomolgus monkeys with PF-06409577 for 6 weeks resulted in a reduction in circulating cholesterol. Together these data suggest that activation of AMPK β1 complexes with PF-06409577 is capable of impacting multiple facets of liver disease and represents a promising strategy for the treatment of NAFLD and NASH in humans.

1. Introduction

Increases in human over-nutrition have expanded the incidence of metabolic disorders and raised the risk of cardiovascular events, causing a significant societal burden. The etiology of the set of conditions that make up this cardio-metabolic syndrome is complex and involves alterations in systemic lipid and glucose metabolism, in addition to cardiovascular and renal diseases. The liver plays a key role in the syndrome as an integrator of the hormonal and metabolic signals that regulate lipid and glucose synthesis and their transit to peripheral tissues (Reccia et al., 2017; Tilg et al., 2017). These hepatic actions are dysregulated in the cardio-metabolic syndrome, with excessive *de novo* production, storage, and trafficking of fatty acids and cholesterol, increasing cardiovascular risk factors and driving non-alcoholic fatty liver disease (NAFLD), non-alcoholic steatohepatitis (NASH), and increasing the likelihood of hepatocellular carcinoma (HCC) (Bril and Cusi, 2017). Pharmaceutical therapies that halt or reverse the hepatic abnormalities associated with this altered metabolic state are needed to lessen the increasing burden of resulting diseases on societies around the world.

The 5′AMP-Activated Protein Kinase (AMPK) has evolved as an important cellular sensor of reduced energy status that can subsequently phosphorylate its target proteins, slowing the rates of key biosynthetic processes and promoting energy producing pathways; for these reasons AMPK has been proposed as a therapeutic target for metabolic diseases (Day et al., 2017; Garcia and Shaw, 2017; Ross et al., 2016). AMPK was initially identified as an enzymatic activity capable of AMP-activated

* Corresponding author at: Pfizer IMRU, 1 Portland Street, Cambridge, MA 02139, USA.
E-mail address: Russell.miller@pfizer.com. (R.A. Miller).

https://doi.org/10.1016/j.ebiom.2018.04.009

phosphorylation and inhibition of two rate limiting enzymes in fatty acid and cholesterol metabolism: Acetyl-CoA Carboxylase (ACC) and HMG-CoA Reductase (HMGCR) (Carling et al., 1987; Yeh et al., 1980). This remarkable evolutionary solution to incorporate energetic regulation to key metabolic pathways has subsequently been shown to have been applied to many more pathways, an ever expanding catalog of AMPK substrates that sit at key regulatory steps in many important pathways, including the master regulator of lipogenic transcription sterol regulatory element binding proteins (SREBP) and the mTOR regulatory proteins TSC2 and Raptor (Gwinn et al., 2008; Inoki et al., 2003; Li et al., 2011).

The understanding of the role AMPK plays in the liver during metabolic disease states has evolved during the last decade of intense research on the kinase. Initial work using indirect pharmacological activators of AMPK (*i.e.* AICAR and metformin) suggested AMPK was capable of dominantly suppressing gluconeogenesis and glucose production (Vincent et al., 1996; Zhou et al., 2001); however more recent work using genetic models of AMPK deficiency or direct pharmacological activators of AMPK indicated that AMPK is not an important regulator of this pathway (Cokorinos et al., 2017; Foretz et al., 2010; Fullerton et al., 2013; Salatto et al., 2017). In contrast to gluconeogenesis, the role of AMPK in regulating fatty acid metabolism has been established with many studies using genetic models of AMPK deficiency alone and in combination with pharmacological activators of AMPK showing that AMPK is important for inhibiting lipogenesis, effects which appear to be largely mediated through inhibitory phosphorylation of ACC (Dzamko et al., 2010; Fullerton et al., 2013; Woods et al., 2017). Importantly, genetic models have established that these changes in AMPK activity and ACC phosphorylation are also important for regulating whole body glucose homeostasis and insulin sensitivity (Fullerton et al., 2013; Woods et al., 2017).

AMPK activation has also been implicated in non-hepatocyte cell types in ways that could benefit the metabolic syndrome, in particular in the setting of NAFLD and NASH. During the transition from simple fatty liver to NASH the non-hepatocyte liver cells drive inflammatory signaling and culminate in damaging fibrosis that results in loss of liver function, with both infiltrating and resident inflammatory cells driving this phenotype (Nati et al., 2016). Importantly, genetic removal of AMPKβ1 in hematopoietic cells *in vivo* increases liver macrophage infiltration and inflammation in obese mice fed a high-fat diet while pharmacological activation of macrophages *in vitro* using the direct AMPK β1 specific activator A769662 suppresses inflammation (Galic et al., 2011). Consistent with these findings, multiple reports using indirect activators of AMPK have implicated AMPK as a suppressor of inflammatory and fibrotic processes in pre-clinical NASH models, although most fail to demonstrate clearly the mechanisms for this benefit (Chen et al., 2017; Lee et al., 2016; Li et al., 2014; Lim et al., 2012; Smith et al., 2016). Additionally, AMPK has been implicated in inhibiting adipose tissue lipolysis in some (Bourron et al., 2010; Daval et al., 2005; Kim et al., 2016) but not all (Mottillo et al., 2016; Yin et al., 2003) studies as well as inducing the browning of white fat (Mottillo et al., 2016), which collectively may serve to reduce hepatic lipids in a cell non- autonomous manner. However, much of this work has used indirect activators of AMPK to evaluate both the site and mechanism by which activation of AMPK could be beneficial as a therapeutic intervention. Therefore, more selective chemical tools are necessary for the rational and precise drug discovery in this pathway that would be necessary for the development of a safe and effective therapeutic.

Recent work has detailed the impact of genetic deletion of AMPK in the liver, revealing only minor phenotypes upon removal in mice (Boudaba et al., 2018). However, these studies very elegantly showed the potential for small molecule-mediated activation of AMPK to elicit large changes in lipid metabolism in hepatocytes. This included increased hepatic fat oxidation and reductions in hepatic lipid and cholesterol synthesis, corroborating other work showing AMPK activation to be a robust inhibitor of anabolic pathways in the liver. These authors also showed that in animals that had elevated *de novo* lipogenesis because of SREBP1 overexpression AMPK activation using a small molecule activator resulted in a striking reduction in hepatic lipids (Boudaba et al., 2018).

In the current study, we use a small molecule activator biased towards AMPK β1 subunits, PF-06409577, in combination with a rodent model that lacks the ability to phosphorylate and inhibit ACC in the liver, to demonstrate the potential for therapeutic benefit in NAFLD and hyperlipidemia. Using both rodent and primate studies, we show that AMPK activation with PF-06409577 is capable of impacting lipid and cholesterol pathways beneficially, suggesting potential for a general improvement in liver health. Our work extends the findings of Boudaba et al. (2018) by studying the impact of AMPK activation in dietary NAFLD models in mice and in primates using a clinically viable small molecule, increasing the expectation of human translation of this line of study.

2. Materials and Methods

2.1. Rodent Studies

All animal experiments were conducted following study protocols and procedures reviewed and approved by Pfizer Institutional Animal Care and Use Committee. The facilities that supported this work are fully accredited by AAALAC International. For mouse studies, 8–10 week old male AMPK $\alpha1^{lox/lox}$ $\alpha2^{lox/lox}$ mice on the C57BL/6J mice were purchased from Jackson Laboratories and maintained on 60% kcal fat diet (Research Diets) for 24 weeks. Mice were housed in a 12 h light:dark cycle. Mice were then infected with 1×10^{11} viral copies of AAV2/8-TBG-GFP or AAV2/8-TBG-Cre virus (University of Pennsylvania Vector Core) by tail vein injection. Two weeks after viral infection animals began to be orally dosed with PF-06409577 or vehicle (0.5% methyl cellulose/0.1% Tween-80) at a dose of 100 mg/kg and a volume of 10 mL/kg. Upon completion of the study animals were anesthetized under isoflurane 4 h after their last compound dose and tissues and plasma were collected and snap frozen for subsequent analysis. Liver and plasma triglyceride and cholesterol were analyzed using the ADVIA® 1800 Clinical Chemistry System (Siemens).

For studies in ZSF1 rats, six week-old, male ZSF-1 lean and ZSF-1 obese rats (Charles River, Wilmington, MA) were acclimated and randomized by body weight and urinalysis. Daily administration of 0.5% methyl cellulose (p.o.), PF-06409577 at 10, 30, or 100 mg/kg (p.o.) was initiated and continued for 67 days. On Day 67 all rats were administered a final dose after 16-hour overnight fasting. Each rat was then anesthetized with isoflurane and liver tissue and terminal blood glucose was collected for subsequent studies.

2.2. Immunoblotting

Liver tissue samples were homogenized in RIPA buffer (50 mM Tris-HCl, pH 8.0, 150 mM NaCl, 1% IGEPAL, 0.5% w/v sodium deoxycholate and 0.1% w/v sodium dodecyl sulfate) with 1 mM phenylmethylsulfonyl fluoride (Thermo Fisher Scientific), protease inhibitor cocktail (Sigma) and Halt's phosphatase inhibitor (Thermo Fisher Scientific). Protein samples were subjected to SDS-PAGE using a 4–15% gradient gel (Bio-Rad), and transferred to a nitrocellulose membrane. Membranes were incubated overnight with primary antibodies against phospho-AMPK (Thr172) (Cell Signaling), phospho-ACC (Ser79) (Millipore), phospho-SREBP-1 (Cell Signaling), AMPK (Cell Signaling), ACC (Cell Signaling), SREBP-1 (BD Biosciences), SREBP-2 (Seo et al., 2011), β-actin (Sigma) and YY-1 (Cell Signaling), followed by HRP-conjugated secondary antibodies and chemiluminescent detection. Immunoblot intensities were quantified using ImageJ analysis software (Rasband, W.S., ImageJ, U. S. National Institutes of Health, Bethesda, Maryland, USA, https://imagej.nih.gov/ij/, 1997–2016).

2.3. MSD Assays

Liver tissue samples were homogenized in cell lysis buffer (Cell Signaling). For AMPK MSD assays Standard Bind plates (Meso-Scale Diagnostics, L15XA-3) were coated overnight at 4 °C with 120 ng/well of AMPKα antibody (Abcam, 80,039). Each well was washed once with 200 μL 1× MSD Tris Wash Buffer (Meso-Scale Diagnostics, R61TX-1) then 200 μL of 1% Blocker A (Meso-Scale Diagnostics, R3AA-2), diluted in 1× Tris Wash Buffer, was added to each well and incubated at 37 °C for 1 h. Wells were washed and 25 μg of the protein samples of interest were added to each well, then incubated at 37 °C for 2 h. Wells were then washed three times with 200 μL of 1× Tris Wash Buffer, then either phospho AMPK antibody (Cell Signaling, 2535) at 25 ng/well or total AMPK antibody (Cell Signaling, 5831) at 100 ng/well, diluted in 1% MSD Blocker A, were added to respective wells and incubated for 1.5 h at 37 °C. Wells were then washed with 1× Tris Wash Buffer, once, then 50 ng of MSD Sulfo-Tag antibody (Meso-Scale Diagnostics, R32AB-1) was added to each well and incubated at 37 °C for 1 h. Wells were washed three times with 1× Tris Wash Buffer, 150 μL of 1× MSD Read Buffer (Meso-Scale Diagnostics, R92TC-2) was added to each well and plate read on an MSD plate reader (Meso-Scale Diagnostics, Sector S600).

For ACC MSD assays, MSD Streptavidin gold plates (Meso-Scale Devices, L15SA-2) were blocked in 1% Blocker A (Meso-Scale Diagnostics, R3AA-2), diluted in 1× Tris Wash Buffer, and incubated at 37 °C for 1 h. Following incubation, wells were washed three times with 200 μL of 1× Tris Wash Buffer, 25 μg of the protein samples of interest were added to each well, then incubated at 37 °C for 2 h. Wells were then washed three times with 200 μL of 1× Tris Wash Buffer, then either phospho ACC antibody (Millipore, 07–303) at 50 ng/well or total ACC antibody (Cell Signaling, 3676) at 25 ng/well, diluted in 1% Blocker A, were added to respective wells and incubated for 1.5 h at 37 °C. Wells were then washed with 1× Tris Wash Buffer, once, then 50 ng of MSD Sulfo-Tag antibody (Meso-Scale Diagnostics, R32AB-1) was added to each well and incubated at 37 °C for 1 h. Wells were washed three times with 1× Tris Wash Buffer, 150 uL of 1× MSD Read Buffer (Meso-Scale Diagnostics, R92TC-2) was added to each well and plate read on an MSD plate reader (Meso-Scale Diagnostics, Sector S600).

2.4. In vitro AMPK Assays

AMPK allosteric activation and/or protection from dephosphorylation was determined as previously reported (Cameron et al., 2016).

2.5. Cell Based Assays

Primary rat hepatocytes were isolated and plated in 96 well plates at a density of 35,000 cells/well in Williams E Media for studies the following day. Cryopreserved human (Corning) or cyno monkey hepatocytes (Thermo Fisher Scientific) were plated at a density of 35,000 cells/well in Williams E Media for studies the following day. For phospho-ACC measurements cells were treated with compounds for 1 h and lysed in cell lysis buffer for subsequent MSD ELISA measurements (as described above). For *de novo* lipogenesis measurements, cells were treated with compounds for 1 h followed by treatment with compound and supplemented with 0.8 μCi ^{14}C-2-acetic acid (ARC0158B, American Radiolabeled Chemicals) and incubated (37 °C, 5% CO_2) for 1 h. After final incubation, experimental media was removed and 50 μL Cell Lytic MEM Protein Extraction (Sigma, CE0050) added to each well then placed in −80 °C freezer until processing. For processing, lysates were thawed on ice then 150 μL Microscint E (Perkin Elmer, 6013661) added to each condition than 200 μL transferred to a 96-well Isoplate (Perkin Elmer, 6005040) for counting.

2.6. DNL and Cholesterol Synthesis Assays

Lipogenesis methodology was adapted from previous publications. Briefly, primary mouse hepatocytes were isolated and plated overnight in Williams E Media (WEM) supplemented with 10% FBS, 1% antibiotic and 2 mM glutamine. Cells were serum starved for 2 h and then treated with experimental compounds in the presence of ^{3}H acetate in serum free WEM for 4 h. Cells were washed and snap frozen in 1 mL of 1 M KOH/EtOH. Cells were then scraped and wells rinsed with another 1 mL of 1 M KOH/EtOH and transferred into glass vials for saponification. Samples were vortexed and then heated for 2 h at 70 °C. Following samples reaching room temperature, 1 mL of H_2O and 2 mL of n-hexane was added to the glass vial, vortexed, and then centrifuged for 5 min (1500 rpm) at room temperature. Top phase was then added to scintillation vial for counting of the sterol fraction. 1 mL of 2 N HCl and 2 mL of petroleum ether were added to the bottom phase. This solution was vortexed and then centrifuged for 5 min (1500 rpm) at room temperature. The top phase was then added to a scintillation vial for counting of the fatty acid fraction.

Primary hepatocytes were generated from ACC-DKI (Fullerton et al., 2013) and hepatocyte-specific AMPK knockout mice and fatty acid and sterol synthesis assessed, respectively, as previously described (Fullerton et al., 2013; Pinkosky et al., 2016).

2.7. Gene Expression Analysis

Mouse livers were homogenized in Qiazol (Qiagen) and RNA was isolated using RNeasy Mini Kit (Qiagen) following manufacturer's protocol. RNA was quantified using Nanodrop 2000 and converted to cDNA using Applied Biosystem's High Capacity cDNA Reverse Transcription Kit (Thermo Fisher Scientific) following manufacturer's protocol. Gene expression was measured using TaqMan Gene Expression Assay. Library preparation for RNA-seq was performed as previously described (Cokorinos et al., 2017).

For RNA sequencing samples, RIN values determined using an Agilent 2200 Tapestation (Agilent, G2964AA) and RNA ScreenTape (Agilent, 5067-5576) to ensure optimal quality with values of seven or greater used in library preparation. RNA library preparation performed according to manufacturer supplied protocol for TruSeq® Stranded mRNA LT - Set A-B (Illumina, RS-122-2101-RS-122-2102) kits. Following library preparation, fragment distribution (Agilent, 5067-5584) and quantification (Kapa, KK4835) performed to ensure optimal library quality. Libraries were then diluted and pooled for single-end read sequencing performed using NextSeq 500/550 High Output v2 kit (75 cycles) (Illumina, FC-404-2005) on an Illumina NextSeq 500 series sequencer. Raw sequencing reads were demultiplexed using bcl2fastq software. Reads were aligned to the mouse reference genome (mm10) using STAR (v2.4.0) (Dobin et al., 2013). Counts were summarized at the gene level using featureCounts from the Subread package (v1.4.6) and Ensembl gene annotations. Quality was verified using a combination of Picard Metrics and visualization of top principal components. Differential expression testing was performed by fitting a linear model of the effect of treatment on observed counts using the DESeq2 library (v1.10.1) in the R statistical environment (v3.2.4) (Love et al., 2014). Gene set enrichment analysis was performed with the R library GAGE (v2.20.1) using the mouse GO and KEGG annotations provided in the gagedata package (v2.8.0).

2.8. Cynomolgus Monkey Studies

PF-06409577 was administered by oral gavage to cynomolgus monkeys (3/sex/group) once daily for 6 weeks at doses of 0 (vehicle control) or 25 mg/kg/day. A comprehensive evaluation of clinical laboratory measurements was conducted, including total serum cholesterol, triglycerides, HDL and LDL. This study was conducted in accordance with Good Laboratory Practice (GLP) guidelines.

2.9. SILAC HepG2 Cell Culture and Compound Stimulation

Proteomic experiments with AMPK activator PF-06409577 were carried out with triple SILAC labeled HepG2 cells (Ong and Mann, 2007). HepG2 cells were purchased from the American Type Culture Collection (ATCC, Manassas, VA) and cultured in customized high glucose SILAC DMEM media (PAA laboratories, catalog number E15-086) supplemented with 10% dialyzed FBS with 10 K molecular weight cut off (PAA laboratories, catalog number A11-507) and supplemented with penicillin/streptomycin. Extracted proteins were quantified by Bradford method and combined at equal protein concentration (1,1:1 light:medium:heavy). Proteins were separated using 1D-SDS gel and subdivided into 12 gel slices. For each gel slice, proteins were first reduced with dithiothreitol (DTT) and alkylated with iodoacetamide (IAA) before proceeding with trypsin digestion which was carried out at 37 °C for overnight.

Mass spectrometric analyses were carried out with Eksigent nanoLC (Sciex, Framingham, MA) coupled with Elite LTQ-Orbitrap mass spectrometer (Thermo, Bremen, German). Nano-LC column (15 cm × 75 μm) was packed in house using precut silica tubing PicoTip Emitter (New Objective, Woburn, MA) with 3 μm ReproSil-Pur C18 resin (Dr. Maisch, Entringen, Germany).

2.10. Nuclear Fractionation

Nuclear proteins were isolated following fractionation methods as described previously (Roqueta-Rivera et al., 2016). Briefly, the largest lobe of the fresh mouse liver was dissected and immediately minced with a razor blade on a chopping board. Finely minced tissues were transferred to a tube containing 1× PBS with 1 mM phenylmethylsulfonyl fluoride (PMSF) (Thermo Fisher Scientific), protease inhibitor cocktail (Sigma), Halt's phosphatase inhibitor (Thermo Fisher Scientific). Samples were centrifuged at 900 ×*g* for 5 min in 4 °C. Liver pellets were dounce homogenized in homogenization buffer (2 M sucrose, 10% glycerol, 0.15 mM spermine, 25 mM KCl, 1 mM EDTA, 1 mM EGTA, 10 mM HEPES pH 7.6) with protease and phosphatase inhibitors. Samples were centrifuged at 100,000 ×*g* for 1 h in 4 °C. Nuclear pellets were re-suspended in nuclear lysis buffer (50 mM Tris pH 7.6, 500 mM NaCl, 10 mM EDTA) with protease and phosphatase inhibitors. Samples were sonicated using a Bioruptor (Diagenode) and centrifuged at 20,000 ×*g* for 5 min in 4 °C. Supernatant was collected and transferred to a fresh tube. Protein concentrations were determined using BCA protein assay kit (Thermo Fisher Scientific). Nuclear protein samples were subjected to SDS-PAGE using 4–15% gradient gel (Bio-Rad) and transferred to a nitrocellulose membrane.

3. Results

The small molecule AMPK activator PF-06409577 potently activates AMPK heterotrimeric complexes that contain the AMPK β1 subunit (Supplemental Figs. 1A-B) (Cameron et al., 2016). The AMPK β1 subunit is the predominant β subunit isoform in mouse and rat livers, unlike the livers of cynomolgus monkeys and humans which express the AMPK β1 isoform but have relatively higher expression of the AMPK β2 isoform (Supplemental Fig. 1C) (Cokorinos et al., 2017; Stephenne et al., 2011; Wu et al., 2013). We sought to evaluate whether there were sufficient AMPK β1 containing heterotrimers in rodent and primate hepatocytes to derive pharmacological benefit from a biased AMPK β1 activator such as PF-06409577. Despite the varying amounts of AMPK β1, treatment of rat, monkey, or human primary hepatocytes with PF-06409577 resulted in a dose-dependent increase in the phosphorylation of ACC at serine 79, a known AMPK phosphorylation site, with an EC_{50} of 69, 875, or 255 nM for rat, monkey, and human primary hepatocytes (Fig. 1A). Consistent with this increase in ACC phosphorylation, PF-06409577 dose dependently lowered acetate incorporation into lipid (a combined measure of *de novo* lipogenesis and cholesterol synthesis) with an IC_{50} of 49, 444, or 128 nM for rat, monkey, or human primary hepatocytes (Fig. 1B). These data suggested that PF-06409577 would be capable of eliciting pharmacology in a clinical setting in human liver; however, it does suggest that species with lower abundance of AMPK β1 in liver (monkeys and humans) may require higher concentrations of PF-06409577 to elicit the same response as observed in rodents.

Hepatocytes isolated from mice lacking AMPK α subunits were studied to assess the requirement of AMPK for the effects of PF-06409577 on lipogenesis. AMPK $\alpha1^{lox/lox}/\alpha2^{lox/lox}$ mice infected with either AAV-TBG-GFP (WT) or AAV-TBG-Cre (HepKO) were isolated and showed a dramatic reduction in AMPK α subunits, ACC phosphorylation at Serine 79, and stimulation of AMPK or ACC phosphorylation following treatment with 10 μM PF-06409577 (Fig. 2A). In studies of *de novo* lipogenesis PF-06409577 delivered at a concentration of 10 μM was capable of lowering acetate incorporation into the saponifiable lipid fraction in hepatocytes from wild type but not AMPK HepKO mice (Fig. 2B). When acetate incorporation was measured in the non-saponifiable fraction, indicative of sterol synthesis, we observed a reduction of synthesis in hepatocytes from wild-type mice that was only partially blunted in the hepatocytes from AMPK HepKO mice (Fig. 2C). To examine the specificity of PF-06409577 to inhibit fatty acid synthesis through AMPK inhibition of ACC, hepatocytes were isolated from mice that lacked the key inhibitory AMPK phosphorylation sites on ACC1 (Ser79Ala) and ACC2 (Ser212Ala) (ACC-DKI mice). In hepatocytes from ACC-DKI mice, the effect of PF-06409577 to acutely suppress fatty acid (Fig. 2D) was blunted relative to wild-type controls.

PF-06409577 is orally bioavailable and has appropriate pharmacokinetic properties for use in rodents, allowing us to evaluate its impact on lipid and cholesterol biosynthesis *in vivo* (Cameron et al., 2016). PF-06409577 lowered the incorporation of ^{14}C-acetate into hepatic lipids *in vivo* in a dose dependent manner (Fig. 2E). Plasma mevalonic acid, a direct product of HMGCR, was also shown to be reduced acutely following a single dose of PF-06409577, similar to the HMGCR inhibitor Rosuvastatin (Fig. 2F).

We evaluated PF-06409577 in a rodent model of diet induced metabolic syndrome that lacked AMPK specifically in the hepatocytes, allowing us to understand which drug actions were the result of hepatocyte AMPK activation. AMPK $\alpha1^{lox/lox}/\alpha2^{lox/lox}$ mice were fed a high fat diet for an extended period of 24 weeks prior to infection with adeno-associated virus expressing either GFP or Cre specifically in the hepatocytes. Livers from mice infected with Cre virus (AMPK-HepKO) showed a near complete removal of total and phospho-threonine 172 AMPK alpha protein, as well as a decrease in the levels of the AMPK phosphorylation site on ACC, serine 79 (Fig. 3A), indicating efficient deletion of the AMPK α1 and α2 alleles following viral expression of Cre recombinase. Unbound plasma concentrations of PF-06409577 were measured in these animals and averaged 20 nM 4 h after being dosed. We did not observe a change following AMPK knockout or activation with PF-06409577 in the reported AMPK-mediated phosphorylation site on SREBP1, serine 372 (Fig. 3A).

AMPK HepKO and control mice were both treated with PF-06409577 for either one dose of 100 mg/kg or 42 days of consecutive once daily oral dosing of 100 mg/kg, and sacrificed 4 h after treatment for evaluation of the impact of drug action. PF-06409577 caused AMPK activation after acute (Fig. 3B-C) and chronic dosing (Fig. 3D-E), as determined by measurement of AMPK phosphorylation at Thr172 and ACC phosphorylation at Ser79 using antibody based MesoScale Diagnostics (MSD) assays which function similar to ELISAs. Despite the daily activation of AMPK for 42 days there was no impact of PF-06409577 on body weight, body composition, or glucose and insulin levels before and after a glucose tolerance challenge, results consistent with studies using a similar AMPK β1 biased activator (Supplemental Fig. 2) (Cokorinos et al., 2017).

PF-06409577 had a large impact on hepatic lipids, in contrast to the modest impact on weight and glycemic traits. PF-06409577 treatment resulted in lower hepatic triacylglycerol (TAG) and hepatic cholesterol

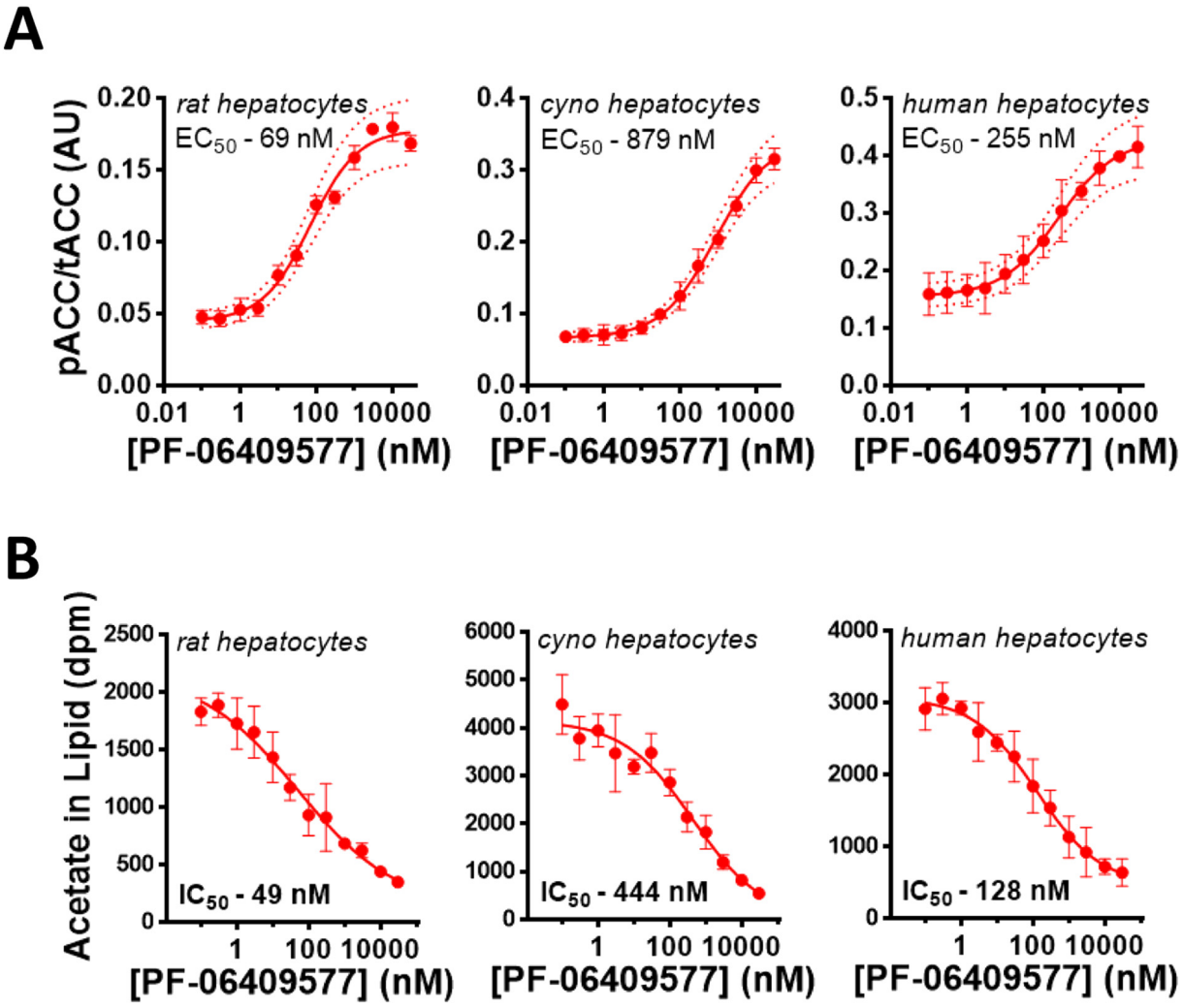

Fig. 1. PF-06409577 increases ACC phosphorylation and suppresses lipid synthesis in primary hepatocytes from rats, monkeys and humans.

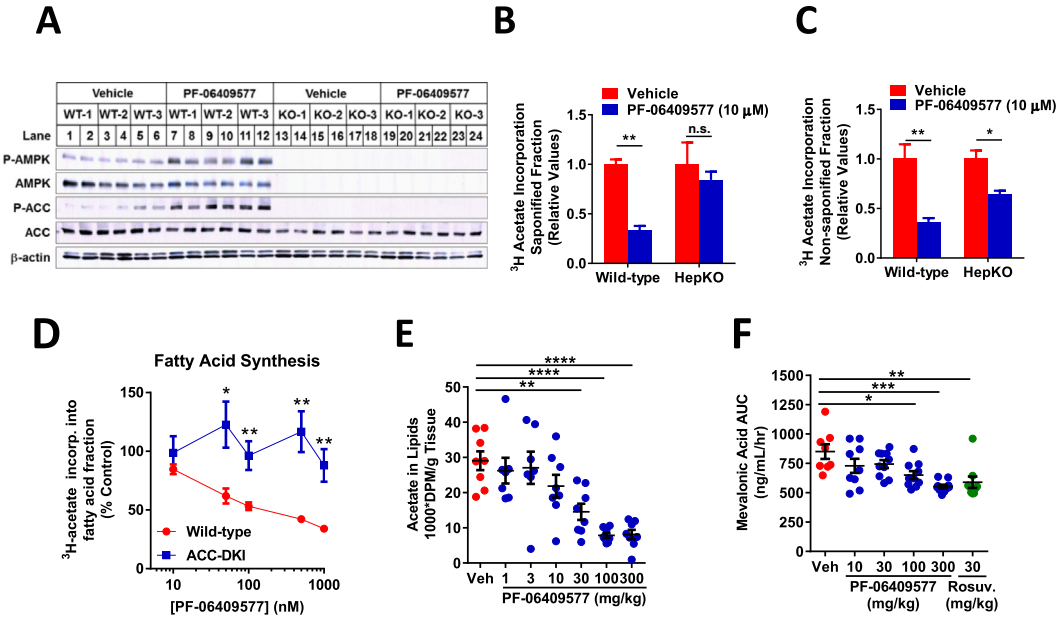

Fig. 2. PF-06409577 requires AMPK activity in order to reduce lipid synthesis in rodent primary hepatocytes and livers.

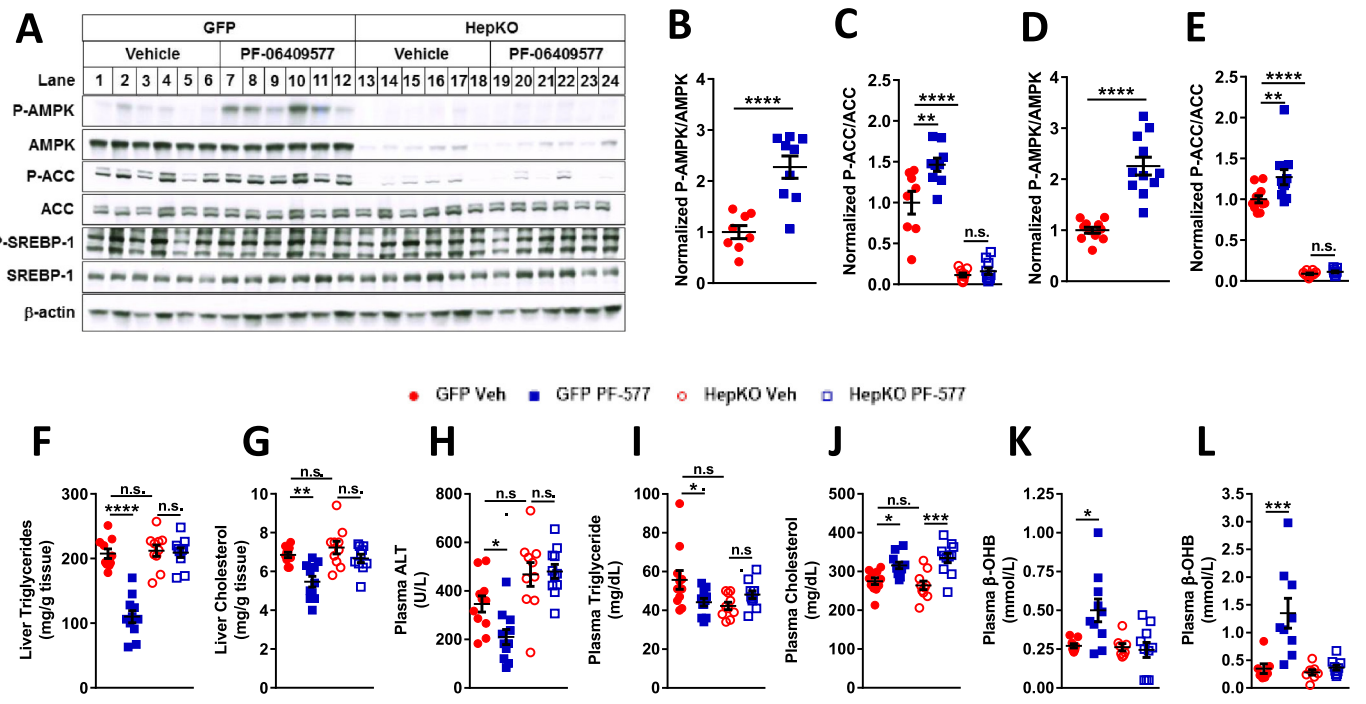

Fig. 3. PF-06409577 acutely and chronically activates AMPK in the liver *in vivo* and reduces liver and plasma triglycerides and increased plasma β-hydroxybutyrate levels.

in the control AAV-GFP infected animals (Fig. 3F-G). In AMPK HepKO animals there was no impact of PF-06409577 on liver TAG or cholesterol (Fig. 3F-G). Staining of liver samples with Oil Red O and histological analysis of stain area confirmed these results (Supplemental Fig. 2I-J). Plasma levels of the alanine liver transaminase (ALT), a marker for general liver health that is elevated in NAFLD and NASH, was also lowered in control AAV-GFP infected animals treated with PF-06409577, but not AMPK HepKO animals, consistent with the general reduction in hepatic lipid content (Fig. 3H). These effects suggested the benefit of PF-06409577 treatment resulted from AMPK activation in hepatocytes and not from other locations such as the adipose tissue or macrophages.

Evaluation of systemic circulating lipids revealed only modest changes following chronic PF-06409577 treatment, in contrast to the large impact on hepatic lipid levels. Nonetheless, a significant reduction in circulating triglycerides was observed following PF-06409577 treatment in control but not AMPK HepKO mice (Fig. 3I). In contrast to small changes in circulating triglycerides, PF-06409577 resulted in a large increase in plasma β-hydroxybutyrate, after 42 days of dosing as

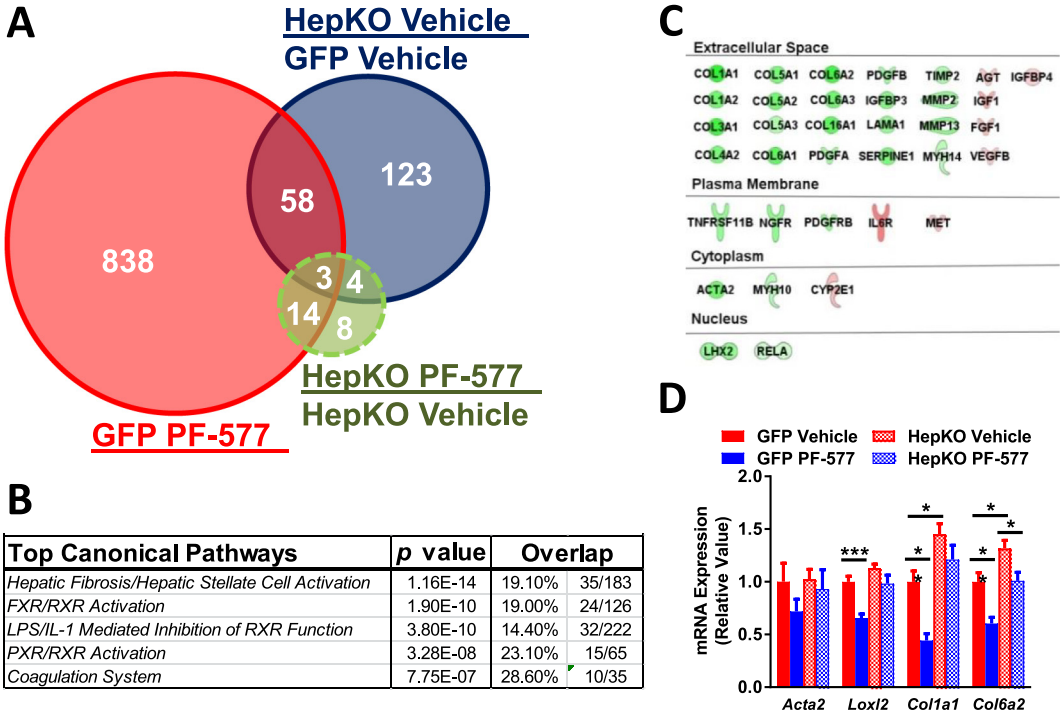

B

Top Canonical Pathways	*p* value	Overlap	
Hepatic Fibrosis/Hepatic Stellate Cell Activation	1.16E-14	19.10%	35/183
FXR/RXR Activation	1.90E-10	19.00%	24/126
LPS/IL-1 Mediated Inhibition of RXR Function	3.80E-10	14.40%	32/222
PXR/RXR Activation	3.28E-08	23.10%	15/65
Coagulation System	7.75E-07	28.60%	10/35

Fig. 4. Chronic treatment of PF-06409577 reduces liver fibrosis in control mice but not in hepatocyte-specific AMPK knockout mice.

well as after a single dose of compound (Fig. 3K-L). PF-06409577 failed to cause a change in circulating β-hydroxybutyrate in HepKO mice, suggesting that the effects were driven by β-hydroxybutyrate production in the hepatocyte (Fig. 3K-L).

An unbiased evaluation of hepatic mRNA was performed to assess the impact of hepatocyte AMPK activation on the transcriptome. The expression of 913 genes were altered in control mice after chronic PF-06409577 treatment, 188 genes were affected by knocking out AMPK in hepatocytes, and expression of 29 genes were altered as a result of PF-06409577 treatment in the AMPK HepKO mice (Fig. 4A). To understand the cellular pathways affected by PF-06409577, we used the Ingenuity pathway analysis (IPA) software, which determined hepatic fibrosis/hepatic stellate cell activation as the main pathway affected by PF-06409577 treatment (Fig. 4B). Within this pathway, PF-06409577 reduced the expression of genes in the collagen family in control but not in AMPK HepKO livers, an effect that was confirmed by qPCR measurements of mRNA levels (Fig. 4C-D).

In addition to markers of fibrosis, transcriptional targets of the SREBP transcription factors and mitochondrial proteins exhibited elevated mRNA in the livers of control mice treated chronically with PF-06409577 (Fig. 5A-B). Changes in SREBP-target genes were not accompanied by changes in SREBP-1 protein or mRNA levels, and we did not observe significant changes in the nuclear form of SREBP-1 or SREBP-2 (Supplemental Fig. 3). Given these paradoxical findings which were in contrast to reports of AMPK inhibition of SREBPs and the reduction in hepatic lipids we had observed, we performed an unbiased evaluation of proteomic changes induced by PF-06409577 in the HepG2 hepatoma cell line. Overnight PF-06409577 treatment caused a number of changes to the proteome (Fig. 5C-E), with a clear induction of SREBP target genes involved in fat and cholesterol biosynthesis (Fig. 5C), consistent with the observed effects in livers of mice treated with PF-06409577 chronically. We also observed a cluster of ribosomal proteins related to mTOR signaling with reduced protein expression (Fig. 5D), and a cluster of mitochondrial proteins (Fig. 5E) that were significantly elevated in HepG2 cells treated with PF-06409577.

These data suggested that AMPK activation was eliciting a robust elevation in SREBP signaling, a result that may be expected given the reduction in hepatic cholesterol biosynthesis secondary to HMGCR inhibition (Goldstein and Brown, 2015). Circulating cholesterol levels were modestly elevated following PF-06409577 treatment, in both AMPK HepKO and control mice (Fig. 3J), suggesting potential for a non-hepatic effect of the compound in this model. However, the normal HFD-fed mouse has a systemic cholesterol profile that is dissimilar to humans, with very low LDL and high HDL cholesterol, making this model's relevance to humans unclear. Because of the complexity of interpreting the circulating cholesterol profile of the HFD-fed mouse we sought a rodent model with a more human-like cholesterol profile. The ZSF1 rat, a cross between a leptin receptor-deficient and hypertensive-heart failure (SHHF) rats, is a cardio-renal model that exhibits hypercholesterolemia but low HDL, similar to humans with hypercholesterolemia (Dower et al., 2017). In chronic studies of PF-06409577 dosed orally at 100, 30, or 10 mg/kg in this model there was a dose-dependent increase in liver AMPK activation (Fig. 6A), with no impact on glycemic measures (Salatto et al., 2017). Chronic treatment with PF-06409577 caused a dose dependent reduction in circulating total cholesterol and non-HDL cholesterol in the plasma, and a dose dependent increase in plasma HDL cholesterol (Fig. 6B-C). Similar to the effects observed in DIO mice, treatment of ZSF1 rats with PF-006409577 was capable of reducing the amount of liver triglycerides following chronic treatment (Fig. 6D).

The lower AMPK β1 subunit expression in the livers and hepatocytes of cynomolgus monkeys and humans as compared to rodents, and requirement for higher drug concentrations to elicit cellular effects, compelled the *in vivo* evaluation of PF-06409577 in monkeys to confirm the

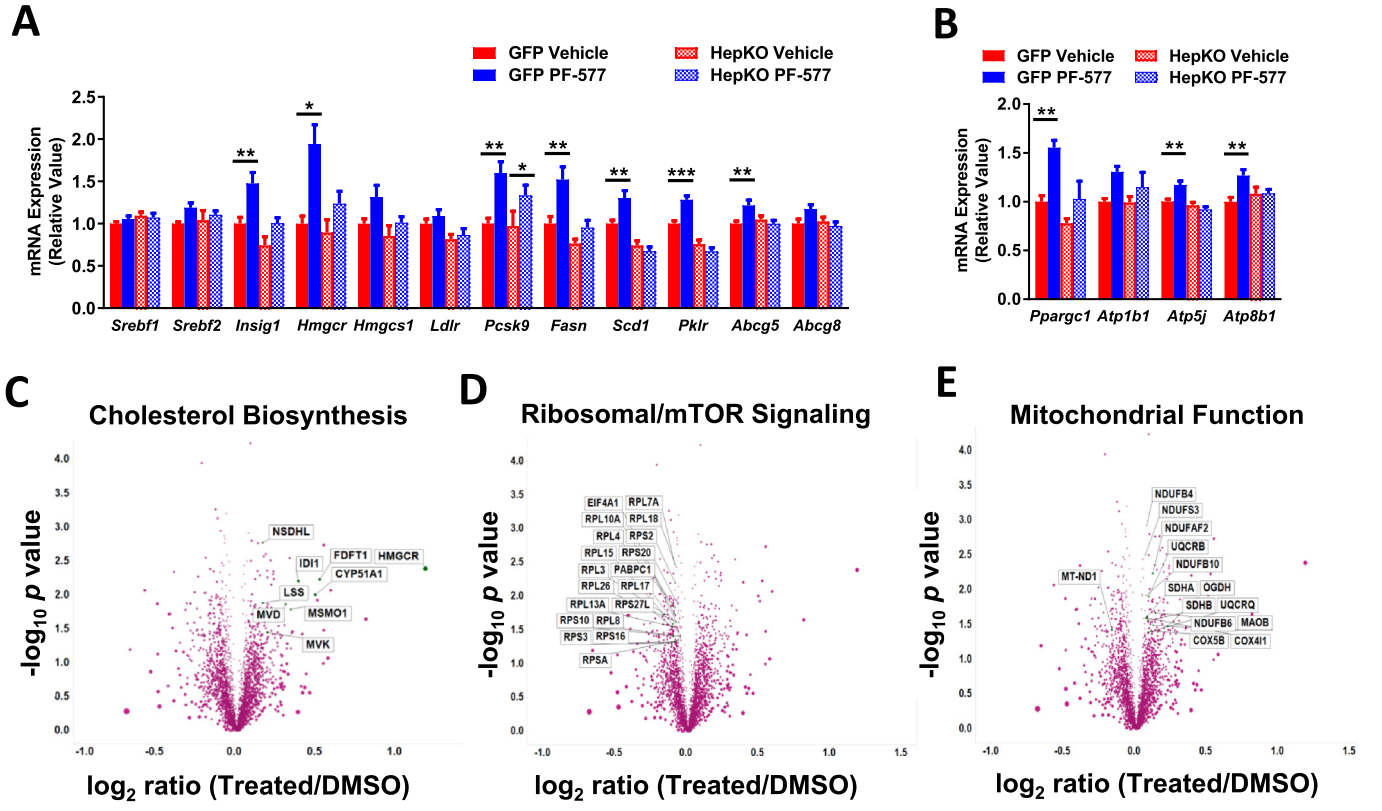

Fig. 5. PF-06409577 increases the expression of genes regulating fatty acid and cholesterol synthesis and mitochondrial function in mouse livers after chronic treatment; and PF-06409577 regulates protein expression involved in cholesterol synthesis and mitochondrial function while suppressing mTOR in cell culture.

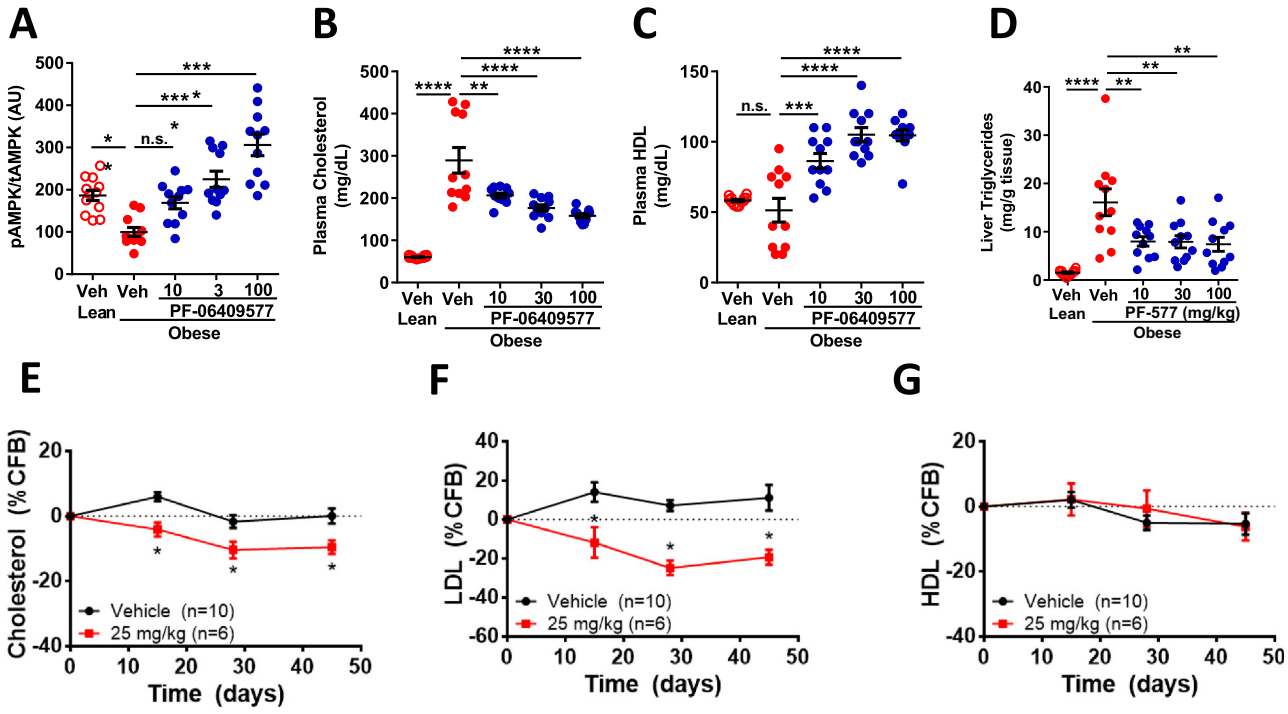

Fig. 6. PF-06409577 results in reduced plasma cholesterol in rats and monkeys.

compound could elicit pharmacology in primates and give confidence in potential for clinically viable efficacy. We evaluated the impact of PF-06409577 on plasma levels of cholesterol, LDL, and HDL during 6 weeks of dosing in cynomolgus monkeys. Cynomolgus monkeys showed a reduction in circulating plasma cholesterol and LDL after 2 weeks of dosing that persisted over the course of the 6 week study (Fig. 6E-F). There was no change in the HDL levels as compared to vehicle treated animals (Fig. 6G).

4. Discussion

Hepatic dysfunction in the metabolic syndrome is a driver of negative patient outcomes that requires more therapeutic options. The complexity of liver alterations in this disease – elevated *de novo* synthesis of fatty acids and cholesterol, reduced clearance of circulating atherogenic LDL, and inflammation and fibrosis that is secondary to steatosis – has proven difficult to treat with single agents. The observation here that pharmacological activation of the energy sensor AMPK, first identified for its actions on lipid and cholesterol pathway enzymes ACC and HMGCR, is capable of such multifactorial impact on the liver in this disease setting is a promising advance. These finding are exciting yet we remain cautious given their preliminary nature; due to the lack of extensive fibrosis development in the DIO and many other mouse NAFLD models and because our observations are based on mRNA expression profiles.

Activation of AMPK has been reported to lower hepatic TAG in multiple studies, yet the exact mechanism for TAG lowering has been unclear because of a large number of potential mechanisms for liver TAG lowering that exist. Here we definitively show that a direct activator of AMPK, PF-06409577, is capable of significant reductions in liver TAG through actions originating in the hepatocytes, and therefore rule out a significant role for non-autonomous control of hepatic lipids driven by changes in adipose lipolysis or signaling through hepatic enervation in this model. The primary mechanisms that have been proposed whereby AMPK can lower hepatic TAG autonomously are the inhibition of ACC to cause reduced *de novo* lipogenesis and increased fatty acid oxidation and inhibition of SREBP-1 transcriptional activity leading to reductions of lipogenic gene expression. Here we show that activation of AMPK results in an increase in the expression of SREBP target genes, and resulting increase in protein levels suggesting that the phosphorylation of ACC predominates over this pathway; a finding consistent with recent studies targeting ACC (Fullerton et al., 2013; Harriman et al., 2016; Kim et al., 2017).

Our studies do not quantitatively evaluate the importance of hepatic fatty acid oxidation and *de novo* lipogenesis in the reductions of hepatic triglyceride. Additionally, our *in vivo* evaluation of PF-06409577 in a high fat fed DIO mouse model, where *de novo* lipogenesis is not as quantitatively important as other models or diabetic humans, suggests that fat oxidation is likely playing a significant role in the hepatic TAG reduction. Our observation of PF-06409577-mediated increases in plasma ketone bodies is consistent with this. PF-06409577 was also capable of robust reductions in liver TAG in the ZSF1 rat, a genetic model that would be expected to have elevated *de novo* lipogenesis. Taken together, these data suggest that AMPK activation with PF-06409577 is capable of lowering hepatic lipids in diverse models and likely through a combination of both inhibition of *de novo* lipogenesis and stimulation of fatty acid oxidation.

The increase in hepatic SREBP target genes, both lipogenic and those in the cholesterol signaling pathway, is contradictory to a previous work suggesting AMPK phosphorylates and inhibits SREBP-1c (Li et al., 2011). However, this effect is consistent with the AMPK-mediated phosphorylation and inhibition of HMGCR or ACC, reducing hepatic cholesterol and plasma mevalonic acid or lipid species, initiating increased processing of the SREBP transcription factors, and an increase in the mRNA of their target genes. In the case of ACC inhibition this has been shown carefully in recent reports describing hepatic knockout and pharmacological inhibition of ACC (Kim et al., 2017). This cascade of events is also triggered by pharmacological inhibitors of HMGCR, the statin class of cholesterol lowering drugs, and results in lower *de novo* cholesterol synthesis and increased LDL clearance because of increases in cell surface LDL-receptor (Goldstein and Brown, 2015). It is also observed with inhibition of lipid synthesis involving pharmacological blockage of ATP citrate

lyase or genetic removal of ACC (Kim et al., 2017; Pinkosky et al., 2016). AMPK activation with PF-06409577 is capable of this ultimate outcome of reduced plasma LDL in two models – cynomolgus monkeys and a rat model of metabolic syndrome – suggesting this is an effect with potential for clinical translation. Although the precise mechanisms underlying this LDL lowering remain to be confirmed, the similarities between pharmacological inhibition of HMGCR with statin-class drugs and phosphorylation-based inhibition of HMGCR with PF-06409577 are evident.

Hepatic inflammation and fibrosis are hallmarks of the NASH phenotype and are thought to occur in a subset of patients with NAFLD. While it is hypothesized that therapeutic lowering of hepatic lipids will be sufficient to improve hepatic fibrosis and inflammation secondarily, this remains controversial and requires more evidence. Here we show that the hepatic actions of PF-06409577, presumably *via* the large reductions in hepatic lipids, are sufficient to reduce molecular indications of hepatic inflammation and fibrosis in a model with developed disease. While it is important to recognize the relatively mild fibrotic and inflammatory liver phenotype of the high fat diet fed DIO mouse, these data are encouraging and suggest that reduced hepatic lipid content can indeed impact this non-hepatocyte cell derived structural liver phenotype secondarily. More work is required to demonstrate this in models of NASH that have more significant degrees of fibrosis.

In vivo, where PF-06409577 was present in the plasma at 20 nM 4 h after being dosed, the compounds effects on hepatic triglycerides and cholesterol levels was completely dependent on the presence of hepatocyte AMPK. In contrast, control and HepKO hepatocytes treated with PF-06409577 at 10 μM were still capable of significantly lowering acetate incorporation into non-saponifiable lipids, a measure of cholesterol synthesis. From the summation of this work we conclude that the *in vivo* actions of PF-06409577 are dependent on liver AMPK, but it is possible that some off-target effects may impact cholesterol synthesis at high concentrations.

Here we show that an activator of AMPK β1 containing heterotrimers elicits robust pharmacological improvement of multiple liver parameters. AMPK β1 heterotrimers are highly expressed in rodent liver but are not the dominant β isoform in human and cynomolgus monkey livers. In cell-based assays this species difference required a significantly higher drug concentration in primate cells to elicit similar downstream effects compared with rodent cells. Importantly, PF-06409577 is capable of eliciting pharmacological effects in cynomolgus monkeys, suggesting there is sufficient AMPK β1 containing heterotrimers in primates to enable pharmacological benefit; however, the levels of drug required to elicit clinically relevant benefit may be higher than that observed in rodent species. The evaluation of this mechanism in humans remains untested or undisclosed, but this work provides some confidence that pharmacological benefit is possible.

Conflicts of Interest

During completion of these studies RME, CTS, JD, BA, AR, YS, RM, EC, MP, MM, JB, EB, CN, KFG, JMK, AO, JW, ASK, JT, LB, NS, MJB, KOC, RAM were employed by Pfizer Inc.

Author Contributions

RME designed and performed mouse studies. CTS designed and performed rat studies. JD and YS performed hepatocyte studies. BA, EC, MP, and EB performed *in vivo* studies. AR and JW designed and performed *in vitro* pharmacology studies. RM performed bioinformatics studies of RNAseq data. MM, CN, and KFG designed and performed proteomic studies. JB performed measures of mevaolnic acid. BS, EAD, and GRS designed and performed studies in ACC DKI hepatocytes. JMK and AO performed histological analyses. ASK and DT evaluated drug metabolism. LB and NS designed and evaluated primate studes. TFO provided key reagents. MJB, KOC, and RAM designed and conceived of studies. RAM wrote the manuscript. All authors provided feedback and edited the manuscript.

A. Phosphorylation of ACC1 S79 and ACC2 S212 (rat) or ACC2 S221 (monkey, human) in rat, monkey and human hepatocytes with increasing amounts of PF-06409577 was quantified by plate based MesoScale Diagnostics (MSD) ELISA-like assays. B. ^{14}C-acetate incorporation into lipids of rat, monkey and human hepatocytes with increasing concentrations of PF-06409577. Assay points are in duplicate and a representative of three experiments is shown.

A. Immunoblots for phospho-AMPK, phospho-ACC, total AMPK, total ACC and β-actin from primary hepatocytes isolated derived from wild-type and liver-specific AMPK deficient (HepKO) mice. Mouse primary hepatocytes were treated with vehicle (DMSO) and PF-06409577 (10 μM) for 1 h. ^{3}H-acetate incorporation into (B) saponified and (C) non-sapanofied lipid fractions within primary hepatocytes derived from wild-type and AMPK HepKO mice. D. ^{3}H-acetate incorporation into fatty acid fraction within primary hepatocytes derived from wild-type and ACC-DKI mice. E. ^{14}C-acetate incorporation into hepatic lipids in rats that were orally dosed with vehicle or PF-06409577. 7–8 animals were used in each dose group. F. Plasma mevalonic acid production from rats that were orally dosed with vehicle, PF-06409577 or rosuvastatin. 8–10 animals were used in each dose group. 1-way ANOVA was used to evaluate statistical significance, where * denotes $p < 0.05$, ** denotes $p < 0.01$, *** denotes $p < 0.001$, and **** denotes $p < 0.0001$.

A. Immunoblots for phospho-AMPK, phospho-ACC, phosho-SREBP-1, total AMPK, total ACC, precursor form of SREBP-1 and β-actin from liver lysates of control (GFP) and liver-specific AMPK deficient (HepKO) mice that were orally dosed vehicle or PF-06409577 (100 mg/kg) 4 h after dosing (acute study). B. Normalized phospho-AMPK levels in GFP mice dosed vehicle or PF-06409577 (PF-577) from single dose acute study measured by MSD assay. C. Normalized phospho-ACC levels in GFP and HepKO dosed vehicle or PF-06409577 from single dose acute study measured by MSD assay. D. Normalized phospho-AMPK levels in GFP mice dosed vehicle or PF-06409577 from 42 day chronic study measured by MSD assay. E. Normalized phospho-ACC levels in GFP and HepKO dosed vehicle or PF-06409577 from 42 day chronic study. 8–11 animals were in each dose group in the studies measured by MSD assay. F. Liver triglycerides of GFP and HepKO mice chronically dosed vehicle or PF-06409577 (100 mg/kg) from 42 day chronic study. G. Liver cholesterol of GFP and HepKO mice dosed vehicle or PF-06409577 (100 mg/kg) from 42 day chronic study. H. Plasma ALT levels of GFP and HepKO mice from 42 day chronic study. (I) Plasma triglyceride,(J) plasma cholesterol and (K) plasma β-hydroxybutyrate of GFP and HepKO mice from 42 day chronic study. L. Plasma β-hydroxybutyrate of mice from acute study. 10–11 animals were in each dose group. 1-way ANOVA was used to evaluate statistical significance, where * denotes $p < 0.05$, ** denotes $p < 0.01$, *** denotes $p < 0.001$, and **** denotes $p < 0.0001$.

A. Venn diagram representing RNA-seq data that show the number of gene overlaps in GFP and HepKO livers after chronic PF-06409577 dosing. B. Top canonical pathways that changed according to Ingenuity Pathway Analysis after chronic PF-06409577 dosing. C. Fibrosis-related genes that were altered in GFP livers after PF-06409577 dosing according to Ingenuity Pathway Analysis. D. qPCR data showing the expression of fibrosis-related genes in GFP and HepKO after chronic PF-06409577 dosing. 5–6 individual animals in each dose group were used in RNAseq analysis. 10–11 animals in each dose group were used in the qPCR analysis. 1-way ANOVA was used to evaluate statistical significance, where * denotes $p < 0.05$, ** denotes $p < 0.01$, *** denotes $p < 0.001$, and **** denotes $p < 0.0001$.

A. qPCR data showing relative expression levels of lipogenic genes in livers from animals treated chronically with PF-06409577. B. qPCR data showing relative expression levels of mitochondria related transcripts in livers of mice treated chronically with PF-06409577. 10–11 animals in each dose group were used for qPCR analysis. C–E. Proteomic analysis

data represented in a volcano plot from HepG2 cells treated vehicle and PF-06409577 overnight, with significant (C) cholesterol biosynthesis, (D) ribosomal/mTOR, and (E) mitochondrial function related protein sets displayed. 1-way ANOVA was used to evaluate statistical significance, where * denotes $p < 0.05$, ** denotes $p < 0.01$, *** denotes $p < 0.001$, and **** denotes $p < 0.0001$.

A-D. ZSF-1 obese rats dosed increasing concentrations of PF-06409577. (A) Normalized hepatic phopho-AMPK levels; (B) plasma cholesterol; (C) plasma HDL and (D) liver triglyceride levels. 10–12 rats were in each dose group. E-G. Cynomolgus monkeys were dosed *p.o.* daily with 25 mg/kg PF-06409577. (E) Plasma cholesterol, (F) plasma LDL, and (G) plasma HDL levels were measured periodically and represented as percent change from each animals baseline value (% CFB). 6–10 monkeys were used in each group. 1-way ANOVA was used to evaluate statistical significance, where * denotes $p < 0.05$, ** denotes $p < 0.01$, *** denotes $p < 0.001$, and **** denotes $p < 0.0001$.

Acknowledgements

G.R.S. is supported by a Canada Research Chair in Metabolism and Obesity and the J. Bruce Duncan Chair in Metabolic Diseases. Experiments in ACC KI mice were supported by grants from the Canadian Institutes of Health Research (125980-1) to G.R.S and mice were provided by Bruce E. Kemp (St. Vincent's Institute of Medical Research, Melbourne Australia).

Appendix A. Supplementary data

Supplementary data to this article can be found online at https://doi.org/10.1016/j.ebiom.2018.04.009.

References

Boudaba, N., Marion, A., Huet, C., Pierre, R., Viollet, B., Foretz, M., 2018. AMPK re-activation suppresses hepatic steatosis but its downregulation does not promote fatty liver development. EBioMedicine 28, 194–209.

Bourron, O., Daval, M., Hainault, I., Hajduch, E., Servant, J.M., Gautier, J.F., Ferre, P., Foufelle, F., 2010. Biguanides and thiazolidinediones inhibit stimulated lipolysis in human adipocytes through activation of AMP-activated protein kinase. Diabetologia 53, 768–778.

Bril, F., Cusi, K., 2017. Management of nonalcoholic fatty liver disease in patients with type 2 diabetes: a call to action. Diabetes Care 40, 419–430.

Cameron, K.O., Kung, D.W., Kalgutkar, A.S., Kurumbail, R.G., Miller, R., Salatto, C.T., Ward, J., Withka, J.M., Bhattacharya, S.K., Boehm, M., et al., 2016. Discovery and preclinical characterization of 6-chloro-5-[4-(1-hydroxycyclobutyl)phenyl]-1H-indole-3-carboxylic acid (PF-06409577), a direct activator of adenosine monophosphate-activated protein kinase (AMPK), for the potential treatment of diabetic nephropathy. J. Med. Chem. 59, 8068–8081.

Carling, D., Zammit, V.A., Hardie, D.G., 1987. A common bicyclic protein kinase cascade inactivates the regulatory enzymes of fatty acid and cholesterol biosynthesis. FEBS Lett. 223, 217–222.

Chen, M., Liu, J., Yang, L., Ling, W., 2017. AMP-activated protein kinase regulates lipid metabolism and the fibrotic phenotype of hepatic stellate cells through inhibition of autophagy. FEBS Open Bio 7, 811–820.

Cokorinos, E.C., Delmore, J., Reyes, A.R., Albuquerque, B., Kjobsted, R., Jorgensen, N.O., Tran, J.L., Jatkar, A., Cialdea, K., Esquejo, R.M., et al., 2017. Activation of skeletal muscle AMPK promotes glucose disposal and glucose lowering in non-human Primates and mice. Cell Metab. 25, 1147–1159 (e1110).

Daval, M., Diot-Dupuy, F., Bazin, R., Hainault, I., Viollet, B., Vaulont, S., Hajduch, E., Ferre, P., Foufelle, F., 2005. Anti-lipolytic action of AMP-activated protein kinase in rodent adipocytes. J. Biol. Chem. 280, 25250–25257.

Day, E.A., Ford, R.J., Steinberg, G.R., 2017. AMPK as a therapeutic target for treating metabolic diseases. Trends Endocrinol. Metab. 28 (8), 545–560.

Dobin, A., Davis, C.A., Schlesinger, F., Drenkow, J., Zaleski, C., Jha, S., Batut, P., Chaisson, M., Gingeras, T.R., 2013. STAR: ultrafast universal RNA-seq aligner. Bioinformatics 29, 15–21.

Dower, K., Zhao, S., Schlerman, F.J., Savary, L., Campanholle, G., Johnson, B.G., Xi, L., Nguyen, V., Zhan, Y., Lech, M.P., et al., 2017. High resolution molecular and histological analysis of renal disease progression in ZSF1 fa/faCP rats, a model of type 2 diabetic nephropathy. PLoS One 12, e0181861.

Dzamko, N., van Denderen, B.J., Hevener, A.L., Jorgensen, S.B., Honeyman, J., Galic, S., Chen, Z.P., Watt, M.J., Campbell, D.J., Steinberg, G.R., et al., 2010. AMPK beta1 deletion reduces appetite, preventing obesity and hepatic insulin resistance. J. Biol. Chem. 285, 115–122.

Foretz, M., Hebrard, S., Leclerc, J., Zarrinpashneh, E., Soty, M., Mithieux, G., Sakamoto, K., Andreelli, F., Viollet, B., 2010. Metformin inhibits hepatic gluconeogenesis in mice independently of the LKB1/AMPK pathway via a decrease in hepatic energy state. J. Clin. Invest. 120, 2355–2369.

Fullerton, M.D., Galic, S., Marcinko, K., Sikkema, S., Pulinilkunnil, T., Chen, Z.P., O'Neill, H.M., Ford, R.J., Palanivel, R., O'Brien, M., et al., 2013. Single phosphorylation sites in Acc1 and Acc2 regulate lipid homeostasis and the insulin-sensitizing effects of metformin. Nat. Med. 19, 1649–1654.

Galic, S., Fullerton, M.D., Schertzer, J.D., Sikkema, S., Marcinko, K., Walkley, C.R., Izon, D., Honeyman, J., Chen, Z.P., van Denderen, B.J., et al., 2011. Hematopoietic AMPK beta1 reduces mouse adipose tissue macrophage inflammation and insulin resistance in obesity. J. Clin. Invest. 121, 4903–4915.

Garcia, D., Shaw, R.J., 2017. AMPK: mechanisms of cellular energy sensing and restoration of metabolic balance. Mol. Cell 66, 789–800.

Goldstein, J.L., Brown, M.S., 2015. A century of cholesterol and coronaries: from plaques to genes to statins. Cell 161, 161–172.

Gwinn, D.M., Shackelford, D.B., Egan, D.F., Mihaylova, M.M., Mery, A., Vasquez, D.S., Turk, B.E., Shaw, R.J., 2008. AMPK phosphorylation of raptor mediates a metabolic checkpoint. Mol. Cell 30, 214–226.

Harriman, G., Greenwood, J., Bhat, S., Huang, X., Wang, R., Paul, D., Tong, L., Saha, A.K., Westlin, W.F., Kapeller, R., et al., 2016. Acetyl-CoA carboxylase inhibition by ND-630 reduces hepatic steatosis, improves insulin sensitivity, and modulates dyslipidemia in rats. Proc. Natl. Acad. Sci. U. S. A. 113, E1796–1805.

Inoki, K., Zhu, T., Guan, K.L., 2003. TSC2 mediates cellular energy response to control cell growth and survival. Cell 115, 577–590.

Kim, S.J., Tang, T., Abbott, M., Viscarra, J.A., Wang, Y., Sul, H.S., 2016. AMPK phosphorylates Desnutrin/ATGL and hormone-sensitive lipase to regulate lipolysis and fatty acid oxidation within adipose tissue. Mol. Cell. Biol. 36, 1961–1976.

Kim, C.W., Addy, C., Kusunoki, J., Anderson, N.N., Deja, S., Fu, X., Burgess, S.C., Li, C., Ruddy, M., Chakravarthy, M., et al., 2017. Acetyl CoA carboxylase inhibition reduces hepatic steatosis but elevates plasma triglycerides in mice and humans: a bedside to bench investigation. Cell Metab. 26, 576.

Lee, H.S., Shin, H.S., Choi, J., Bae, S.J., Wee, H.J., Son, T., Seo, J.H., Park, J.H., Kim, S.W., Kim, K.W., 2016. AMP-activated protein kinase activator, HL156A reduces thioacetamide-induced liver fibrosis in mice and inhibits the activation of cultured hepatic stellate cells and macrophages. Int. J. Oncol. 49, 1407–1414.

Li, Y., Xu, S., Mihaylova, M.M., Zheng, B., Hou, X., Jiang, B., Park, O., Luo, Z., Lefai, E., Shyy, J.Y., et al., 2011. AMPK phosphorylates and inhibits SREBP activity to attenuate hepatic steatosis and atherosclerosis in diet-induced insulin-resistant mice. Cell Metab. 13, 376–388.

Li, J., Pan, Y., Kan, M., Xiao, X., Wang, Y., Guan, F., Zhang, X., Chen, L., 2014. Hepatoprotective effects of berberine on liver fibrosis via activation of AMP-activated protein kinase. Life Sci. 98, 24–30.

Lim, J.Y., Oh, M.A., Kim, W.H., Sohn, H.Y., Park, S.I., 2012. AMP-activated protein kinase inhibits TGF-beta-induced fibrogenic responses of hepatic stellate cells by targeting transcriptional coactivator p300. J. Cell. Physiol. 227, 1081–1089.

Love, M.I., Huber, W., Anders, S., 2014. Moderated estimation of fold change and dispersion for RNA-seq data with DESeq2. Genome Biol. 15, 550.

Mottillo, E.P., Desjardins, E.M., Crane, J.D., Smith, B.K., Green, A.E., Ducommun, S., Henriksen, T.I., Rebalka, I.A., Razi, A., Sakamoto, K., et al., 2016. Lack of adipocyte AMPK exacerbates insulin resistance and hepatic steatosis through Brown and Beige adipose tissue function. Cell Metab. 24, 118–129.

Nati, M., Haddad, D., Birkenfeld, A.L., Koch, C.A., Chavakis, T., Chatzigeorgiou, A., 2016. The role of immune cells in metabolism-related liver inflammation and development of non-alcoholic steatohepatitis (NASH). Rev. Endocr. Metab. Disord. 17, 29–39.

Ong, S.-E., Mann, M., 2007. A practical recipe for stable isotope labeling by amino acids in cell culture (SILAC). Nat. Protoc. 1, 2650–2660.

Pinkosky, S.L., Newton, R.S., Day, E.A., Ford, R.J., Lhotak, S., Austin, R.C., Birch, C.M., Smith, B.K., Filippov, S., Groot, P.H., et al., 2016. Liver-specific ATP-citrate lyase inhibition by bempedoic acid decreases LDL-C and attenuates atherosclerosis. Nat. Commun. 7, 13457.

Reccia, I., Kumar, J., Akladios, C., Virdis, F., Pai, M., Habib, N., Spalding, D., 2017. Non-alcoholic fatty liver disease: a sign of systemic disease. Metabolism 72, 94–108.

Roqueta-Rivera, M., Esquejo, R.M., Phelan, P.E., Sandor, K., Daniel, B., Foufelle, F., Ding, J., Li, X., Khorasanizadeh, S., Osborne, T.F., 2016. SETDB2 links glucocorticoid to lipid metabolism through Insig2a regulation. Cell Metab. 24, 474–484.

Ross, F.A., MacKintosh, C., Hardie, D.G., 2016. AMP-activated protein kinase: a cellular energy sensor that comes in 12 flavours. FEBS J. 283, 2987–3001.

Salatto, C.T., Miller, R.A., Cameron, K.O., Cokorinos, E., Reyes, A., Ward, J., Calabrese, M.F., Kurumbail, R.G., Rajamohan, F., Kalgutkar, A.S., et al., 2017. Selective activation of AMPK beta1-containing isoforms improves kidney function in a rat model of diabetic nephropathy. J. Pharmacol. Exp. Ther. 361, 303–311.

Seo, Y.K., Jeon, T.I., Chong, H.K., Biesinger, J., Xie, X., Osborne, T.F., 2011. Genome-wide localization of SREBP-2 in hepatic chromatin predicts a role in autophagy. Cell Metab. 13, 367–375.

Smith, B.K., Marcinko, K., Desjardins, E.M., Lally, J.S., Ford, R.J., Steinberg, G.R., 2016. Treatment of nonalcoholic fatty liver disease: role of AMPK. Am. J. Physiol. Endocrinol. Metab. 311, E730–E740.

Stephenne, X., Foretz, M., Taleux, N., van der Zon, G.C., Sokal, E., Hue, L., Viollet, B., Guigas, B., 2011. Metformin activates AMP-activated protein kinase in primary human hepatocytes by decreasing cellular energy status. Diabetologia 54, 3101–3110.

Tilg, H., Moschen, A.R., Roden, M., 2017. NAFLD and diabetes mellitus. Nat. Rev. Gastroenterol. Hepatol. 14, 32–42.

Vincent, M.F., Erion, M.D., Gruber, H.E., Van den Berghe, G., 1996. Hypoglycaemic effect of AICAriboside in mice. Diabetologia 39, 1148–1155.

Woods, A., Williams, J.R., Muckett, P.J., Mayer, F.V., Liljevald, M., Bohlooly, Y.M., Carling, D., 2017. Liver-specific activation of AMPK prevents steatosis on a high-fructose diet. Cell Rep. 18, 3043–3051.

Wu, J., Puppala, D., Feng, X., Monetti, M., Lapworth, A.L., Geoghegan, K.F., 2013. Chemoproteomic analysis of intertissue and interspecies isoform diversity of AMP-activated protein kinase (AMPK). J. Biol. Chem. 288, 35904–35912.

Yeh, L.A., Lee, K.H., Kim, K.H., 1980. Regulation of rat liver acetyl-CoA carboxylase. Regulation of phosphorylation and inactivation of acetyl-CoA carboxylase by the adenylate energy charge. J. Biol. Chem. 255, 2308–2314.

Yin, W., Mu, J., Birnbaum, M.J., 2003. Role of AMP-activated protein kinase in cyclic AMP-dependent lipolysis In 3T3-L1 adipocytes. J. Biol. Chem. 278, 43074–43080.

Zhou, G., Myers, R., Li, Y., Chen, Y., Shen, X., Fenyk-Melody, J., Wu, M., Ventre, J., Doebber, T., Fujii, N., et al., 2001. Role of AMP-activated protein kinase in mechanism of metformin action. J. Clin. Invest. 108, 1167–1174.

Author/s:
Esquejo, RM; Salatto, CT; Delmore, J; Albuquerque, B; Reyes, A; Shi, Y; Moccia, R; Cokorinos, E; Peloquin, M; Monetti, M; Barricklow, J; Bollinger, E; Smith, BK; Day, EA; Nguyen, C; Geoghegan, KF; Kreeger, JM; Opsahl, A; Ward, J; Kalgutkar, AS; Tess, D; Butler, L; Shirai, N; Osborne, TF; Steinberg, GR; Birnbaum, MJ; Cameron, KO; Miller, RA

Title:
Activation of Liver AMPK with PF-06409577 Corrects NAFLD and Lowers Cholesterol in Rodent and Primate Preclinical Models.

Date:
2018-05

Citation:
Esquejo, R. M., Salatto, C. T., Delmore, J., Albuquerque, B., Reyes, A., Shi, Y., Moccia, R., Cokorinos, E., Peloquin, M., Monetti, M., Barricklow, J., Bollinger, E., Smith, B. K., Day, E. A., Nguyen, C., Geoghegan, K. F., Kreeger, J. M., Opsahl, A., Ward, J. ,... Miller, R. A. (2018). Activation of Liver AMPK with PF-06409577 Corrects NAFLD and Lowers Cholesterol in Rodent and Primate Preclinical Models.. EBioMedicine, 31, pp.122-132. https://doi.org/10.1016/j.ebiom.2018.04.009.